Journal of Iron and Steel Research, International 24 (2017) 1115—1124

Contents lists available at ScienceDirect

Journal of Iron and Steel Research, International

journal homepage: www.chinamet.cn

Microstructure evolution and mechanical properties influenced by austenitizing temperature in aluminum-alloyed TRIP-aided steel

Ju-hua Liang[1], Zheng-zhi Zhao[1,*], Cai-hua Zhang[2], Di Tang[1], Shu-feng Yang[3], Wei-ning Liu[4]

[1] Collaborative Innovation Center of Steel Technology, University of Science and Technology Beijing, Beijing 100083, China

[2] Technology Center, HBIS Handan Iron and Steel Group Co., Ltd., Handan 056015, Hebei, China

[3] School of Metallurgical and Ecological Engineering, University of Science and Technology Beijing, Beijing 100083, China

[4] AC Construction Branch, State Grid Corporation of China, Beijing 100031, China

ARTICLE INFO

Key words:
Retained austenite
Aluminum
Phase transformation
High strength steel
Mechanical property

ABSTRACT

The Fe-0.21C-2.2Mn-0.49Si-1.77Al transformation induced plasticity (TRIP)-aided steel was heat treated at various austenitizing temperatures under both TRIP-aided polygonal ferrite type (TPF) and annealed martensite matrix (TAM) processes. The microstructure evolution and their effects on mechanical properties were systematically investigated through the microstructure observation and dilatometric analysis. The microstructure homogeneity is improved in TPF steel heated at a high temperature due to the reduced banded martensite and the increased bainite. Compared with the mechanical properties of the TPF steels, the yield strength and elongation of the TAM steels are much higher, while the tensile strength is lower than that of TPF steels. The stability of intercritical austenite is affected by the heating temperature, and thus the following phase transformation influences the mechanical properties, such as the bainite transformation and the precipitation of polygonal ferrite. Obvious dynamic bainite transformation occurs at TAM850, TAM900 and TAM950. More proportion of polygonal ferrite is found in the sample heated at 950 ℃. The bainite transformation beginning at a higher temperature results in the wider bainitic ferrite laths. The more proportion of polygonal ferrite and wide bainitic ferrite laths commonly contribute to the lower strength and better elongation. The uniform microstructure with lath-like morphology and retained austenite with high average carbon content ensures a good mechanical property in TAM850 with the product of strength and elongation of about 28 GPa · %.

1. Introduction

Environmental-friendly materials have always been popular by automotive steel companies. In order to ensure the complex shape for the automotive structures and the lightweight for the fuel economy, a desirable combination of high strength and good formability of automotive steels is indispensable. Metastable retained austenite with transformation induced plasticity (TRIP) effect is an ideal phase in highly deformable high strength steels. Thus, medium manganese lightweight steels have been actively developed[1-4]. Although the lightweight element Al provides a new idea for vehicle light weight, a high content of Al in steel without the Mn matching leads to poor mechanical property. For the consideration of cost advantage and process feasibility, the low-alloy TRIP-aided steels with the low manganese system is more suitable for the existing cold rolled automobile steels. In the past research, an excellent combination of strength and stretch-formability has been found in TRIP-aided multiphase (TMP) steel by Sugimoto[5-11]. Researches[12,13] commonly focused on the composition, austempering temperatures and the types of different matrix morphologies. Nevertheless, the effects of austenitizing temperatures on the mechanical properties are of little concern. Taking into account that the Al element can significantly expand the intercritical temperature range and the process window, the aluminum-alloyed TRIP-aided steel was designed. The effects of austenitizing temperature on the microstructure and mechanical properties of Al-alloyed TRIP-aided steel are studied by comparing the two different matrix morphologies.

* Corresponding author. Prof., Ph.D.
E-mail address: *zhaozhzhi@ustb.edu.cn* (*Z.Z. Zhao*).

Received 31 May 2017; Received in revised form 7 September 2017; Accepted 8 September 2017
Available online 15 November 2017

2. Experimental Procedure

The ingots of 25 kg laboratory smelted steel were forged into several rectangular ingots (60 mm×100 mm×100 mm). The ingots were reheated to roughly 1200 ℃ for 2 h and hot rolled to 4.5－5.0 mm with the coiling temperature of 650 ℃. After pickling, the hot-rolled sheets were directly cold rolled to a thickness of about 1.5 mm. The precise composition is: Fe-0.21C-2.2Mn-0.49Si-1.77Al (wt. %). Rectangular specimens of 70 mm in width and 220 mm in length were machined from the cold-rolled steel sheet parallel to the rolling direction prepared for the heat treatment. The phase volume fraction varying with the heating temperature is theoretically obtained from the appropriate database TCFE7 shown in Fig. 1. Both TRIP-aided annealed martensite type with annealed martensite matrix (TAM) and TRIP-aided polygonal ferrite type (TPF) with polygonal ferrite matrix are designed and prepared for the comparative study. The rectangular sample with annealed martensite matrix, taking into account the possible kinetic factors, was obtained by pre-quenching from 1100 ℃ in a resistance furnace. Surface grinding was done to remove the decarburization layer and the oxide layer. Subsequently, five small rectangular specimens with dimensions of 20 mm × 100 mm were subjected to subsequent heat treatment on the

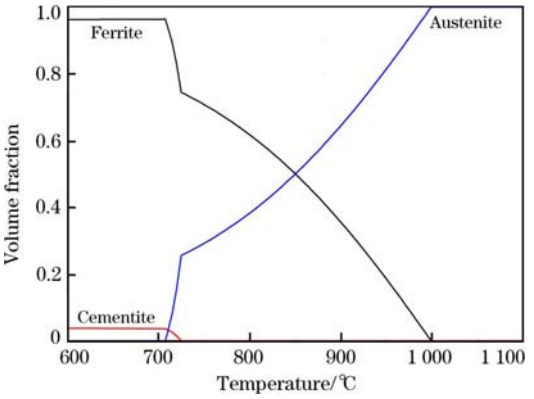

Fig. 1. Phase volume fraction varying with heating temperature.

continuous annealing simulator (CCT-AY-Ⅱ produced by Ulvac-Riko INC). Five different heating temperatures (750, 800, 850, 900 and 950 ℃), combined with the theoretical data were chosen for different phase proportions. The samples were heated at a heating rate of 10 ℃/s to the selected temperature, followed by cooling at 15 ℃/s to 400 ℃ for 5 min and then quenched to room temperature by 50 ℃/s. Another rectangular sample with polygonal ferrite matrix was processed with the same heat treatment parameter. Schematic of the heat treatment cycle is shown in Fig. 2.

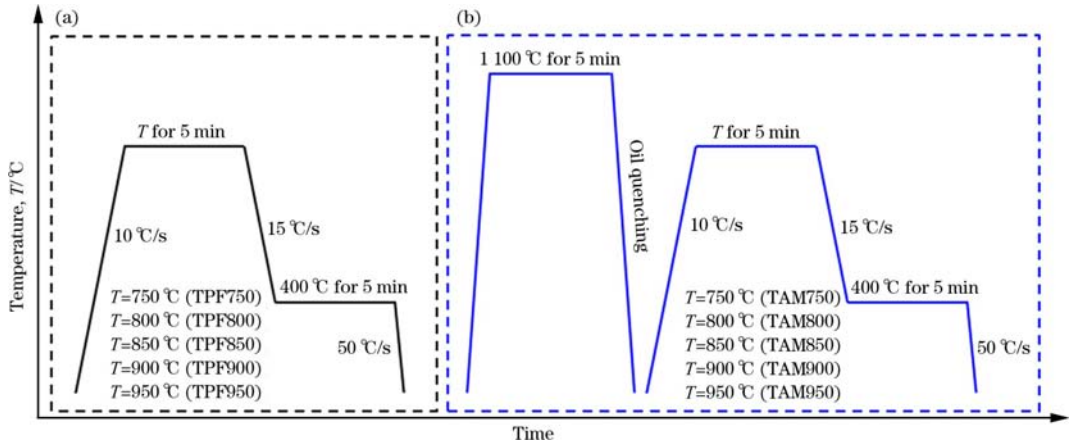

(a) TPF; (b) TAM.

Fig. 2. Schematic diagram of heat treatment procedure.

The dilatometric tests were carried out simultaneously using the same heat treatment parameters in order to analyze the phase transformation process. Thus, the specimens with dimensions of 4 mm×10 mm were machined from the rectangular specimens (70 mm×200 mm). Tensile properties were estimated by the uniaxial tensile test with the gauge length of 25 mm. The tests were performed with a crosshead speed of 1.0 mm/min at room temperature. The resulting microstructures were observed by Zeiss ULTRA 55-type field emission scanning electron microscopy (FE-SEM) after etching with 2 vol. % nital. Electron backscatter diffraction (EBSD) was performed on the samples with 20 kV and a step size of 2 μm. EBSD data were processed with Channel 5 software provided by Oxford HKL technology. X-ray diffraction (XRD) was used to measure the retained austenite fraction and estimate the carbon content of austenite. XRD was performed on the specimen (10 mm×20 mm) at room temperature using the D/MAX-RB operating at 45 kV and 150 mA, the 2θ containing the three FCC peaks ({200}, {220} and {311}) and two BCC peaks

({200}, {211}) scan with the step size of 1° using CuKα radiation. The average carbon concentration of the austenite was approximately obtained by detecting austenite lattice parameter[14-16]. The surfaces of the samples for EBSD and XRD were electrolytically polished with a negligible internal stress in a mixture reagent of 20 vol. % perchloric acid and 80 vol. % ethanol with the voltage of 15 V for 20－30 s.

3. Results and Discussion

3.1. Microstructure observation

The banded microstructures exist in all the five TPF steel samples (as shown in Fig. 3). Microstructure of the conventional TPF steel consists of polygonal intercritical ferrite, bainitic ferrite, retained austenite and the fresh martensite. Although the five minutes intercritical annealing in this study may not lead to the equilibrium in Thermos-Calc, the trend of intercritical ferrite fraction as a function of temperature can be referred to the theoretical data from Thermo-Calc. Thus, the ferrite proportion should be declining with the increasing temperature. Compared with TPF750, the proportion of ferrite in TPF800 decreased indeed. However, at a higher temperature of 950 ℃, higher proportions of polygonal ferrite are significant. This is due to the austenite decomposition during cooling in TPF950, which will be further discussed in the next part of dilatometric analysis.

The microstructure homogeneity is gradually improved with the temperature varying from 750 to 950 ℃. Almost only martensite islands and blocky retained austenite can be observed in the sample of TPF750 except for the intercritical ferrite. With the increasing heating temperature, the proportion of martensite islands or blocky retained austenite in the microstructure decreases continuously. More lath-like bainitic ferrite and fine retained austenite are observed in TPF950 than the others due to the lower average austenite composition. Besides, only a few large martensite islands or blocky retained austenite are sporadically distributed at the prior austenite grain boundaries of sample TPF950. It can be considered that the formation of bainite transformation is inhibited in these areas due to the enrichment of carbon and manganese elements. Similar phenomenon about the elements enrichment at the prior austenite grain boundary also appears in the authors' previous study[14].

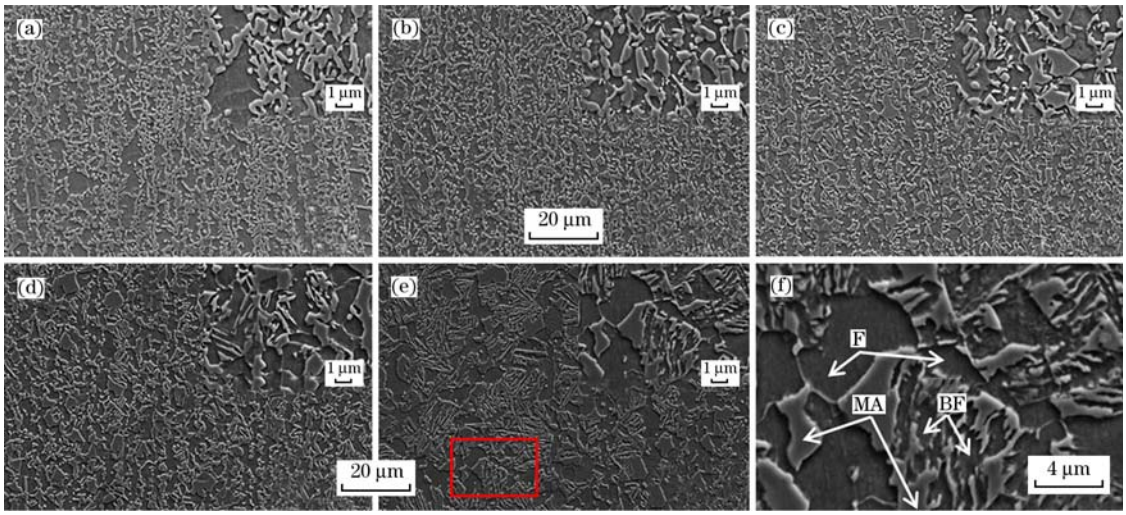

(a) TPF750; (b) TPF800; (c) TPF850; (d) TPF900; (e) TPF950; (f) Partially enlarged for (e).
F—Polygonal ferrite; MA—Blocky martensite or retained austenite; BF—Bainitic ferrite.

Fig. 3. SEM microstructures of TPF steel at different heating temperatures.

Different from the TPF steel, the microstructure of TAM steel (as shown in Fig. 4) exhibits the lath-like morphology inherited from the martensite matrix. The microstructure of TAM steel mainly consists of lath-like intercritical ferrite, bainitic ferrite and the martensite or retained austenite between the laths. Due to the high austenitizing temperature about 1100 ℃, the large prior austenite grain size influences the quenching martensite, resulting in the long length of the martensite lath. In the subsequent intercritical austenitizing and austempering process, the microstructural inheritance also ensures the long length of both intercritical ferrite and bainitic ferrite. Another three points are particularly noteworthy: Firstly, the sample TAM750 has the lowest ferrite proportion in the five samples. Secondly, the width of bainitic ferrite lath in TAM800 is significantly lower than the TAM850 and TAM900. However, the width of bainitic ferrite lath is refined again with the heating temperature rising to 950 ℃. Thirdly, a few polygonal ferrite grains mainly distributed at the prior

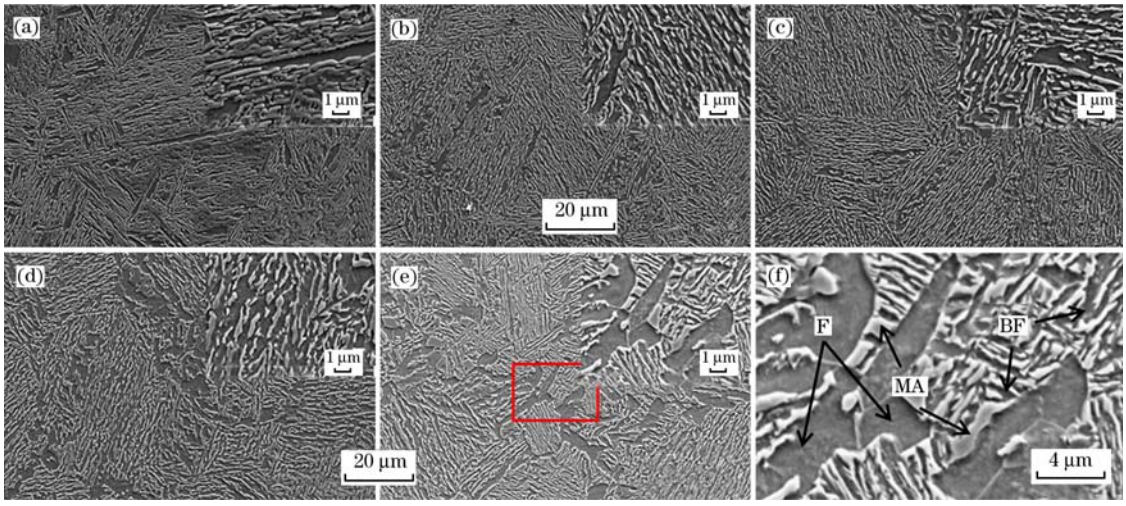

(a) TAM750; (b) TAM800; (c) TAM850; (d) TAM900; (e) TAM950; (f) Partially enlarged for (e).

Fig. 4. SEM microstructures of TAM steel at different heating temperatures.

austenite grain boundaries or martensite packet boundaries are observed in both TAM900 and TAM950. Combining the following dilatometric curves, the reason for these phenomena is not difficult to be found.

3.2. Dilatometric analysis

Dilatometric curves recorded (as shown in Fig. 5) help to have a better understanding of the microstructures of both TPF and TAM steel. As shown in Fig. 5(a,b), the boundary of the partial austenitization in both TPF and TAM aluminum-alloyed steel is blurred from dilatometric curves. Changes in the amount of austenite during heating and holding process can be estimated by the amount of expansion changes, based on the law of leverage. The length of the line segment AB may represent the generation of austenite during heating, and the length of the line segment AC can represent the total austenite fraction after the five minutes intercritical annealing process. The lengths of all lines are listed in Fig. 5(a, b). Although the absolute difference in the amount of expansion between TPF and TAM steel is large, this is mainly due to the different matrix types. The amount of expansion with the temperature trend is consistent.

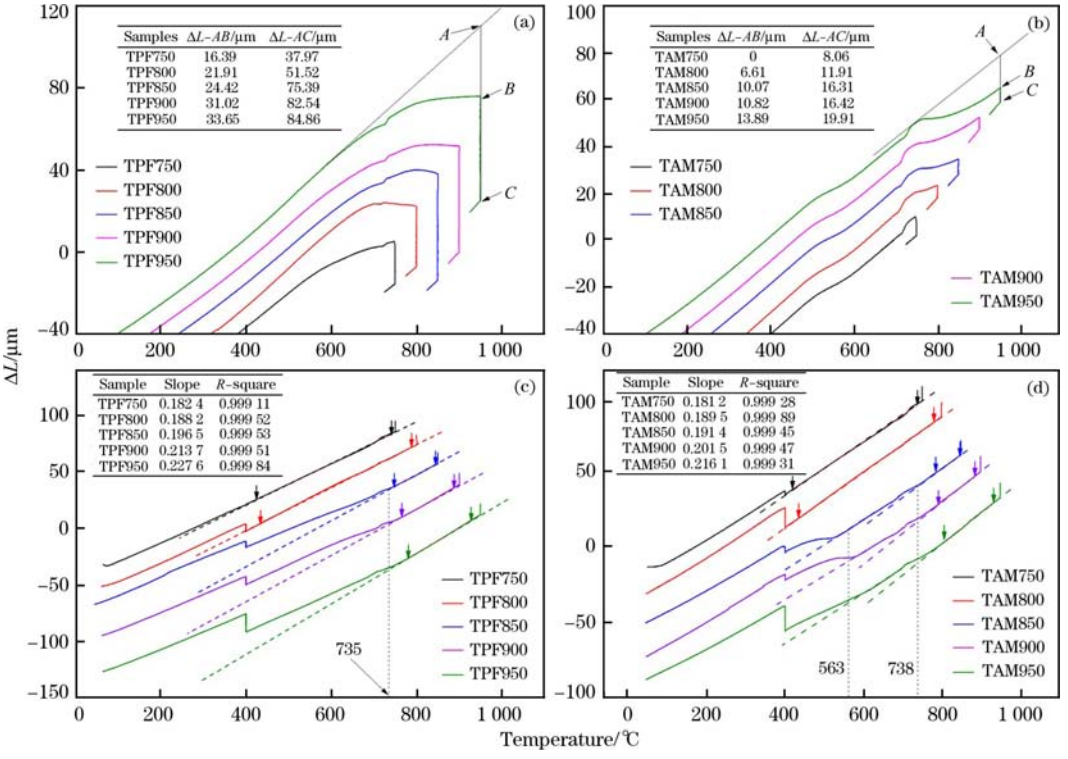

Fig. 5. Dilatometric curves recorded during heating, holding (a, b) and cooling (c, d) sections.

The increasing length of AC proves the indeed declined intercritical ferrite fraction with the rising temperature.

Besides, taking into account the difference between the ferrite and austenite thermal expansion coefficient, there will be different composite expansion coefficients in the initial stage of the cooling process before the phase transformation. Thus, the linear fitting method was used to fit the data points between the arrows in Fig. 5(c, d). R-square values above 0.999 ensure the accuracy of the fit. The resultant slope of each sample during the cooling process is also listed in Fig. 5(c, d). As the temperature rises, the slope exhibits the same regularity, changing from 0.1824 to 0.2276 in TPF steels and from 0.1812 to 0.2161 in TAM steels. This is consistent with the data in Fig. 5(a, b), and the intercritical austenite proportion indeed increases by experimental validation again with the rising temperature.

For the phenomena of microstructure observation in both TPF and TAM steels, the dilatometric curves were analyzed to understand the austenite decomposition during cooling. Higher ferrite proportions in TPF950 can be interpreted by one detail on the dilatometric curve. The polygonal ferrite forms during subsequent cooling process, since the cooling rate is set at 15 ℃/s. Different degrees of polygonal ferrite formation in the samples TPF850, TPF900 and TPF950 can be observed in the cooling process before bainite transformation. In contrast, there is no formation of polygonal ferrite in the samples TPF750 and TPF800 during cooling process. The lower heating temperature in intercritical region, making the carbon and manganese elements more concentrated in the austenite, results in the higher stability of austenite in the following cooling process and the inhibition of polygonal ferrite transformation.

The dilatometric curve has barely changed during the isothermal process at 400 ℃ of TPF750, which means that bainite transformation has been inhibited. In contrast, the martensite transformation can be observed at 90 ℃ in the subsequent cooling process. Besides, with the increasing temperature, the bainite transformation is more and more significant. The dilatometric curve of samples also shows a gradually increasing expansion during the isothermal process at 400 ℃. These phenomena are consistent with the microstructure morphology in Fig. 3.

The phenomenon about the lowest ferrite proportion in TAM750 (Fig. 4) is mainly due to lowest bainitic ferrite proportion, although it has the highest intercritical ferrite fraction. The bainitic ferrite proportion of each sample in TAM steel is also discussed based on dilatometric curves. Similar to the TPF750, little bainite transformation happens in TAM750. The lowest slope of 0.1812 indicates the highest intercritical ferrite fraction in TAM750, which means the most enrichment of carbon and manganese elements in intercritical austenite. Thus, the bainite transformation is inhibited, and the proportion of bainite ferrite in TAM750 is lower than others. It is also proved by the slight expansion of dilatometric curve in TAM750 during the holding time at 400 ℃. The higher expansion amount in TAM800 confirms the further bainite transformation, which means the more proportion of bainitic ferrite and accounts for the higher total ferrite fraction than TAM750.

The phenomenon about width difference of bainitic ferrite laths can also be explained by the dilatometric curves. As shown in Fig. 5(b), there is single expansion site in the dilatometric curve of TAM800 at the austempering temperature of 400 ℃. In contrast, a continuously dynamic expansion process occurs at a higher temperature about 573 ℃ of TAM850, TAM900 and TAM950, which means that the bainite transformation begins at a higher temperature in these three samples. Thus, the microstructure exhibits the different lath widths of bainitic ferrite. Bainitic ferrite formed at the higher temperature has the wider width. For convenience, the bainitic ferrites in TAM steels are artificially divided into two types, bainitic ferrite formed at 400 ℃ and bainitic ferrite formed above 400 ℃. Based on the dilatometric curves, the fraction of each bainitic ferrite can be roughly calculated by the law of leverage. Obviously, the bainitic ferrites of TAM800 are all formed at 400 ℃ with the fine width, while no more than about 25% bainitic ferrite formed at 400 ℃ exists in both TAM850 and TAM900. The essential reason of the different phenomena is the composition difference in intercritical austenite. That is, the relatively higher austenite stability in TAM800 than that in TAM850 and TAM900 inhibits the bainite transformation above 400 ℃ with the cooling rate of 15 ℃/s. Thus, a large number of fine bainitic ferrite laths are formed during holding at 400 ℃. When it comes to the sample TAM950, a few polygonal ferrites formed along the prior austenite grain boundaries during the cooling process, confirmed by both microstructure observation and dilatometric curve. Thus, austenite stability is enhanced by the further enrichment of carbon and manganese elements from the polygonal ferrites. More bainite transformation (about 65%) of TAM950 occurs at lower temperature, so the bainitic ferrite laths are refined again.

3.3. Further analysis for retained austenite and martensite

It is difficult to distinguish the martensite and retained austenite only by SEM observation. Due to the difference in crystallographic parameters be-

tween martensite and retained austenite, the face-centered cubic retained austenite is easily recognized by means of EBSD. In addition, the martensite under EBSD observation has a poor recognition rate due to the higher dislocation density itself, and thus it commonly appears dark on the band contrast map. Further analysis has been performed on microstructure of both TPF steels and TAM steels by fine EBSD observation, as shown in Figs. 6 and 7. The retained austenite fraction and carbon content are also measured by XRD, as shown in Fig. 8.

The banded martensite of TPF800 can be clearly seen along the rolling direction. The banded structure becomes less pronounced as the heating temperature increases. At a higher temperature of 950 ℃, no banded martensite is observed. As the intercritical austenite grains grow due to the increase in heating temperature, the large austenite grains cover the tiny segregation banding. Thus, the banded martensite islands are significantly reduced as shown in Fig. 6. Microstructure homogeneity is greatly improved.

Analyzing the data of XRD in Fig. 8, the retained austenite fraction reaches a value of 8.7% in TPF750, while it decreases to the lowest value of 5.8% in TPF800. The higher intercritical ferrite fraction in TPF750 accounts for the higher retained austenite frac-

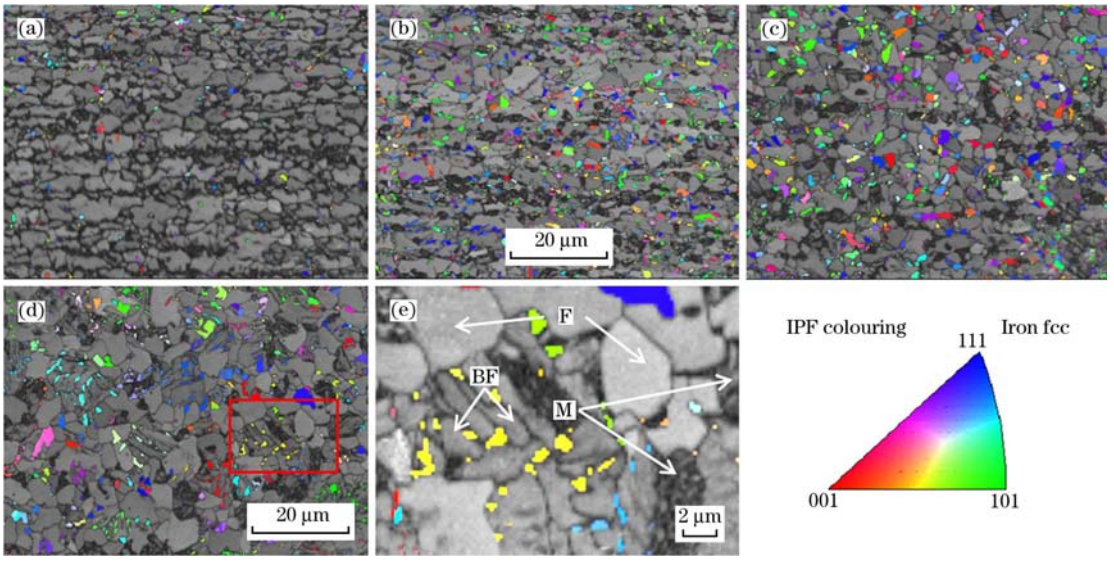

(a) TPF800; (b) TPF850; (c) TPF900; (d) TPF950; (e) Partially enlarged for (d).

Fig. 6. EBSD maps of TPF steels at different heating temperatures, combined band-contrast map of BCC and orientation map of retained austenite. Inset shows inverse pole-figure map for austenite phase.

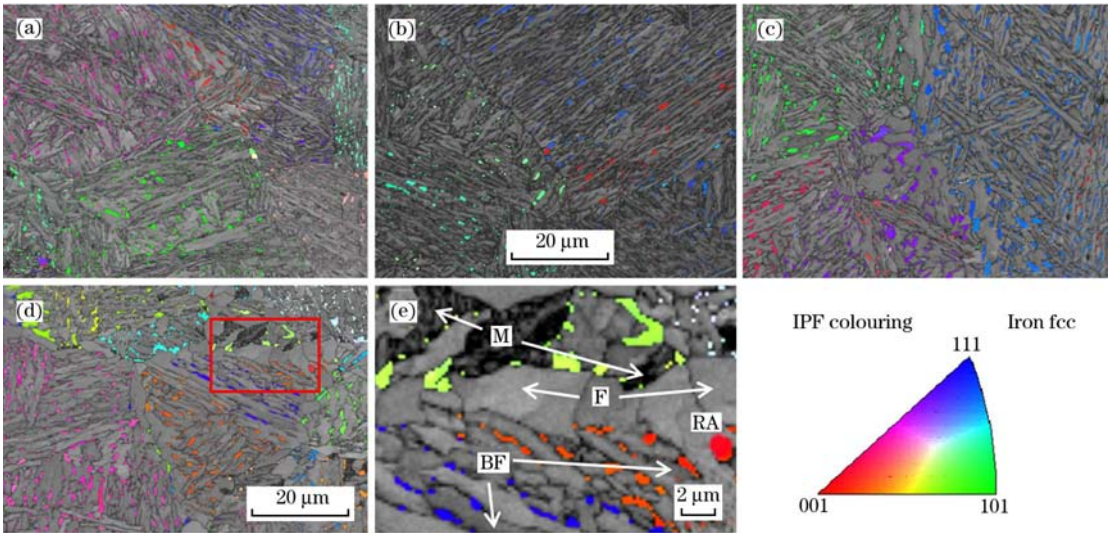

(a) TAM800; (b) TAM850; (c) TAM900; (d) TAM950; (e) Partially enlarged for (d).
M—Martensite; RA—Retained austenite.

Fig. 7. EBSD maps of TAM steels at different heating temperatures, combined band-contrast map of BCC and orientation map of retained austenite. Inset shows inverse pole-figure map for austenite phase.

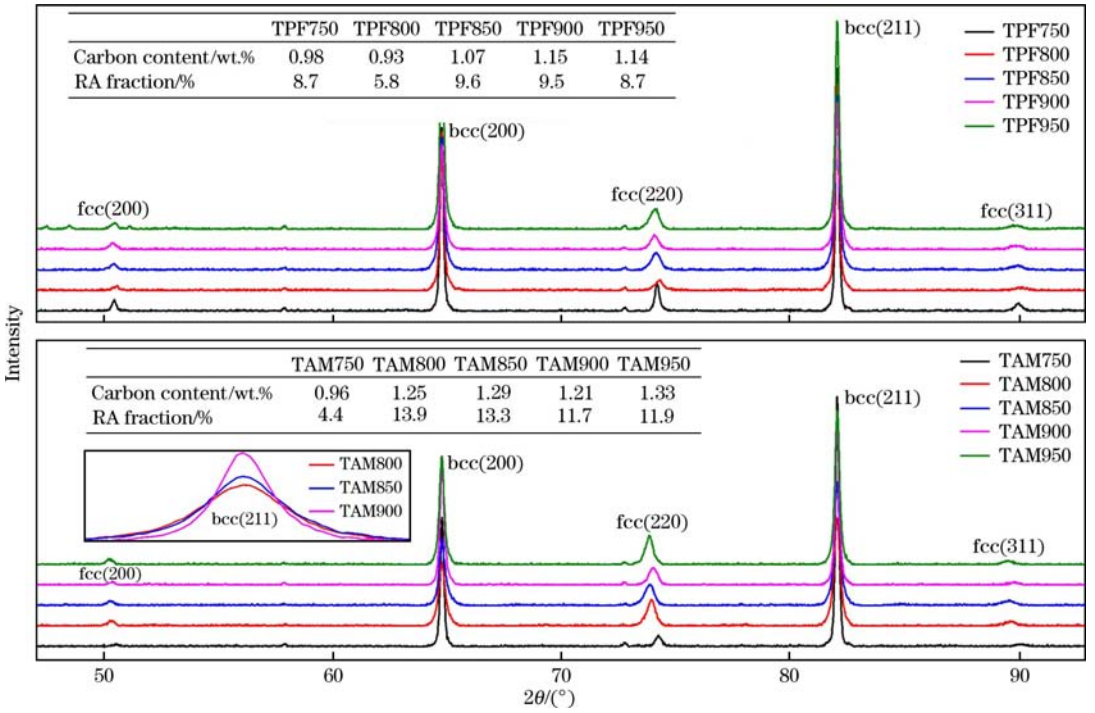

Fig. 8. XRD patterns and data (both retained austenite fraction and carbon content) of investigated steels.

tion than that in TPF800. Then, it develops with the rising temperature in TPF steels. The EBSD results in Fig. 6 show the same regularities. The retained austenite fraction is remarkably improved as the heating temperature increases. At the low temperature of 800 ℃, there is almost no retained austenite, while the retained austenite content basically maintains at a high level with the heating temperature over 850 ℃. Besides, the morphology evolution of retained austenite in TPF steels is also significant. The proportion of blocky retained austenite declines, while the proportion of lath-like retained austenite between the bainitic ferrite increases significantly, especially the retained austenite in TPF950. Furthermore, the average carbon content of the retained austenite is lifted from 0.93% in TPF800 to 1.14% in TPF950. The sufficient bainite transformation during the cooling contributes to the high average carbon content in retained austenite.

Different from the TPF steels, the retained austenite fraction in TAM steel always maintains a high content from the low temperature of 800 ℃ to the high temperature of 950 ℃. In addition, the average carbon content of retained austenite in each sample also maintains a high level except for TAM750 from XRD data. No martensite is observed in the TAM steels except for TAM950. The phenomenon that the large martensite islands only appear at the high temperature of 950 ℃ can be understood from two aspects. On one hand, the intercritical austenite laths are partially merged at the prior austenite grain boundaries of the pre-quenching martensite from 1100 ℃, and thus the large blocky austenite formed. On the other hand, the polygonal ferrite precipitated along the prior austenite grain boundary during the cooling process leads to the local enrichment of the carbon and manganese elements in the vicinity of the austenite interface. Thus, the formation of bainite transformation is inhibited in these areas during austempering process, and it is easy to generate large fresh martensite during the subsequent quenching process as shown in Fig. 7(e). In addition, the phenomenon about width difference of bainitic ferrite laths can also be proved by XRD data, as shown by the inset in Fig. 8. The average grain size of ferrite can be roughly compared by comparing full widths at half-maximum of the ferrite peak (211) in XRD on ubiquitous Scherrer formula[17]. TAM800 has the finest ferrite lath as it has the biggest full width at half-maximum, while ferrite lath of TAM900 is wider than the other two because of its smallest full width at half-maximum.

3.4. Mechanical properties

The mechanical properties and engineering stress-strain curves are listed in Fig. 9. It has been confirmed that different annealing temperatures affect the partial austenitization and subsequent phase transformation process through the microstructural observation and dilatometric analysis. Thus, the mechanical properties are affected by the final microstructure. The yield strength in these steels is generally influenced by the soft phases, such as intercritical ferrite, polygonal ferrite, bainitic ferrite and

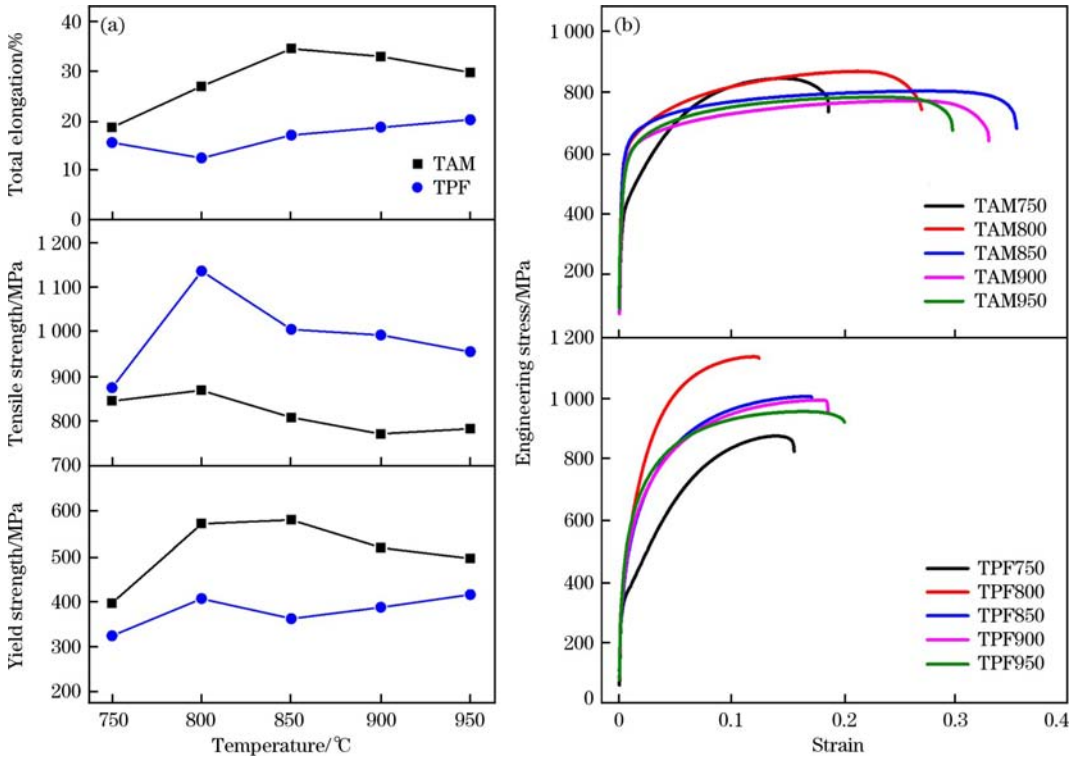

Fig. 9. Mechanical properties (a) and engineering stress-strain curves (b) of both TPF and TAM steels.

so on, while the tensile strength is mainly determined by hard phases both the bainite and martensite. The elongation is affected by a variety of factors, including soft and hard phases. In addition, the microstructural morphology, homogeneity, amounts of retained austenite and its carbon content in various heat treatment conditions also play the key roles.

3.4.1. Mechanical properties of TPF steels

Yield strength of TPF steels generally increases with the rising heating temperature, as the proportion of intercritical ferrite decreases. However, the precipitation of polygonal ferrite during the cooling process with the cooling rate of 15 ℃/s complicates the evolution of mechanical properties, proved by both dilatometric curves (Fig. 5) and microstructure observations (Figs. 3 and 6). For example, compared with TPF800 (406 MPa), the yield strength of TPF850 (362 MPa) slightly decreases. The yield strength is together affected by two competing mechanisms. On one hand, the yield strength value is enhanced with the decrease in the proportion of intercritical ferrite. On the other hand, the formation of polygonal ferrite during cooling in TPF850 reduces the yield strength of the material. As shown in Fig. 9, it is obvious that the decrease caused by the precipitation of polygonal ferrite in TPF850 counteracts the increase affected by change of intercritical ferrite fraction. With the further rise of temperature, the reduction of intercritical ferrite once again dominates the yield strength, leading to a further increase in yield strength.

According to the dilatometric curves and EBSD maps of the TPF750 and TPF800 samples, there is no polygonal ferrite formation during the cooling process and little bainite transformation happened in the austempering. Tensile strength is significantly increased from 875 to 1135 MPa, as the microstructure is basically determined by the martensite fraction in TPF750 and TPF800. Although the proportion of intercritical austenite increases with the further increase of heating temperature, the overall tensile strength of the TPF steel is reduced (from 1005 MPa of TPF850 to 956 MPa of TPF950) and the elongation is improved (from 17.0% of TPF850 to 20.1% of TPF950) by four possible reasons. Firstly, the presence of polygonal ferrite decreases the strength and enhances the ductility of the material. Secondly, the microstructural homogeneity is improved by weakening the banded microstructure and contributing to the increase of the elongation. Thirdly, the amount of bainite increases while the proportion of fresh martensite islands decreases in TPF850, TPF900 and TPF950. Thus, the blocky retained austenite transformed into lath-like morphology, and sufficient bainite transformation contributes to the high average carbon content of retained austenite. Both of them make higher stability of retained austenite promoting sustained TRIP effect and high elongation[18-23]. At last, banded martensite

islands are reduced, as the large intercritical austenite grains cover the tiny segregation banding in TPF steel at a high heating temperature. The improved microstructure homogeneity is also beneficial to the comprehensive mechanical properties.

3.4.2. Mechanical properties of TAM steels

Unlike the TPF steels, the microstructure homogeneity is significantly improved by the presence of the pre-quenching process in the TAM steels. Therefore, in the subsequent intercritical austenitizing process, there is no band-like feature of the microstructure. The yield strength is mainly decided by the lath-like ferrite. In the TAM steels, the lath-like ferrite is mainly composed of two different types. The first is the ferrite formed during the intercritical austenitizing process, and the second is the ferrite formed during the cooling both polygonal ferrite and bainitic ferrite. The yield strength of TAM750 is only dominated by intercritical ferrite, which has a low dislocation density. Therefore, the sample TAM750 exhibits very low yield strength of 397 MPa. The proportion of intercritical ferrite in TPF800 decreases, while the bainitic ferrite dominates the yield strength. Then, the yield strength of TPF800 is significantly elevated with the value of 573 MPa. With the further increase of heating temperature, the homogenization of intercritical austenite internal composition reduces its stability. Thus, the bainite dynamic transformation begins at the higher temperature above 400 ℃, that is, the width of bainitic ferrite lath in higher temperature becomes wider. The yield strength of TAM900 is reduced again with the value of 520 MPa. Besides, a few polygonal ferrites formed in TAM900 also contribute to the low yield strength. Although the width of bainitic ferrite laths is refined again in sample TAM950, the ferrite precipitated during the cooling process once again dominates the yield strength of the material, and the yield strength reaches the value of 495 MPa.

The tensile strength of the TAM steels is mainly affected by the interaction of hard-phase and the retained austenite. Obviously, the bainite transformation in TAM750 as shown in Fig. 5 is slight, and the martensite transformation at the low temperature (about 90 ℃) indicates the little retained austenite fraction of 4.4% in TAM750. As a consequence, it is hard for TAM750 to provide a TRIP effect to sustain the high strength and elongation, although the sample TAM750 has the highest proportion of martensite. According to the dilatometric curves and XRD data, bainite transformation happens at the lower temperature, contributing to the finer bainitic ferrite laths in TAM800 than in TAM850. This is also reflected on the strength difference. Considering the similar retained austenite fraction and carbon content in both TAM800 and TAM850, it can be concluded that the width difference of bainitic ferrite laths is more important rather than the difference from retained austenite. That is, wider bainitic ferrite laths of TAM850 are more conducive to a better elongation. The sample TAM850 exhibits good mechanical properties with the tensile strength of 810 MPa and elongation of 34.5%. The observed decline in tensile strength of TAM900 and TAM950 can be understood in terms of the polygonal ferrite fraction. It should also be noted that the large martensite islands in TAM950 (as shown in Fig. 7(e)) are harmful to the elongation.

In addition, compared with the TPF steels, the yield strength and elongation of the TAM steels are much higher, while the tensile strength is lower than that in TPF steels. It comes mainly from the microstructural differences between the TPF steels and TAM steels. Significant martensite islands can be observed in all of the TPF steels. In contrast, the microstructure in TAM steels essentially consists of bainite and ferrite. Moreover, the higher retained austenite fraction and average carbon content are also conducive to good overall properties in TAM steels.

It is noteworthy that the mechanical property differences between TPF750 and TAM750 are negligible. Similar microstructure of fresh martensite and little retained austenite with low stability leads to the close tensile strength and poor elongation. According to the dilatometric curves, no bainite phase transformation happens in both of them at this temperature. That is, the intercritical ferrite is dominant in terms of the yield strength. While the yield strength under the TAM process is slightly higher, and two possible causes can account for this phenomenon. Firstly, it is difficult to grow nuclei of the intercritical austenite in the barren region in TPF750, due to the presence of elemental segregation banding, while more austenite nucleation positions can be easily provided in TAM750 because of its martensite matrix even in the barren region. Therefore, intercritical austenite fraction is obviously different at the same heating temperature between TPF steels and TAM steels. As shown in Figs. 4(a) and 5(a), the proportion of intercritical ferrite in TPF750 is notably lower than that in TAM750. The less proportion of intercritical ferrite in TAM750 contributes to the higher yield strength. Secondly, the massive ferrite grains gather in the barren region of carbon and manganese, allowing the easy deformation in TPF750. While the ferrite laths will be geometrically constrained by the surrounding martensite in TAM750 with the improved microstructure homogeneity[24]. In terms of TPF950 and TAM950, similar microstructural morphologies account for the close properties, both of which are composed of po-

lygonal ferrite along the prior austenite grain boundary, lath-like bainitic ferrite, retained austenite and fresh martensite islands. The difference in mechanical properties is mainly due to the different proportions of each phase.

4. Conclusions

The Fe-0.21C-2.2Mn-0.49Si-1.77Al TRIP-aided steel was heat treated at various austenitizing temperatures under both TPF and TAM process. The partial austenitization and the subsequent austenite decomposition were detected though the microstructure observation and dilatometric analysis. The influences of austenitizing temperature on mechanical properties were systematically investigated by analyzing microstructure evolution, including intercritical ferrite, bainite, fresh martensite and retained austenite. Different heating temperature leads to the difference of intercritical austenite composition, which affects the subsequent polygonal ferrite formation process and the bainite phase transformation process. In addition, microstructural morphology and homogeneity also play the key role in properties. The specific conclusions of the study are as follows.

(1) In TPF steels, banded martensite islands are reduced, with the temperature varying from 750 to 950 ℃, as the large austenite grains cover the tiny segregation banding. Besides, sufficient bainite transformation results in both stable retained austenite with high average carbon content and improved microstructure homogeneity, which contributes to the overall mechanical property.

(2) In TAM steels, high average alloy composition of the intercritical austenite in TAM750 suppresses the formation of polygonal ferrite and the transformation of bainite. With the rising heating temperature, dynamic bainite transformation happens in TAM850, TAM900 and TAM950. It results in the wider bainitic ferrite laths and lower tensile strength than that in TAM800. In addition, some polygonal ferrite grains in TAM950 may result in the enrichment of elements at partial austenite grain boundaries, which is not conducive to the subsequent bainite transformation and detrimental to elongation.

(3) Compared with the mechanical properties of the TPF steels, the yield strength and elongation of the TAM steels are much higher, while the tensile strength is lower than that in TPF steels. The martensite matrix in TAM steels leads to lath-like microstructural morphology, improving the microstructural homogeneity. The uniform microstructure with lath-like morphology and retained austenite with high average carbon content ensures a good mechanical property in TAM850 with the product of strength and elongation of about 28 GPa · %.

Acknowledgment

This research was funded by National Natural Science Foundation of China (51574028).

References

[1] C. H. Seo, K. H. Kwon, K. Choi, K. H. Kim, J. H. Kwak, S. Lee, N. J. Kim, Scripta Mater. 66 (2012) 519-522.
[2] S. Y. Han, S. Y. Shin, H. J. Lee, B. J. Lee, S. Lee, N. J. Kim, J. H. Kwak, Metall. Mater. Trans. A 43 (2011) 843-853.
[3] S. Lee, B. C. De Cooman, Metall. Mater. Trans. A 45 (2014) 6039-6052.
[4] M. I. Latypov, S. Shin, B. C. De Cooman, H. S. Kim, Acta Mater. 108 (2016) 219-228.
[5] K. Sugimoto, M. Kobayashi, A. Nagasaka, S. Hashimoto, ISIJ Int. 35 (1995) 1407-1414.
[6] K. Sugimoto, A. Kanda, R. Kikuchi, S. Hashimoto, T. Kashima, S. Ikeda, ISIJ Int. 42 (2002) 910-915.
[7] K. Sugimoto, B. Yu, Y. Mukai, S. Ikeda, ISIJ Int. 45 (2005) 1194-1200.
[8] K. Sugimoto, J. Tsuruta, Y. Mukai, Tetsu-to-Hagane 96 (2010) 29-35.
[9] K. Sugimoto, D. Fiji, N. Yoshikawa, Procedia Eng. 2 (2010) 359-362.
[10] H. Tanino, M. Horita, K. Sugimoto, Metall. Mater. Trans. A 47 (2016) 2073-2080.
[11] K. Sugimoto, H. Tanino, J. Kobayashi, Mater. Sci. Eng. A 688 (2017) 237-243.
[12] J. Kobayashi, N. Yoshikawa, T. Murakami, K. Sugimoto, Tetsu-to-Hagane 98 (2012) 610-617.
[13] T. Hojo, J. Kobayashi, K. Sugimoto, Mater. Sci. Technol. 32 (2016) 1035-1042.
[14] Z. Z. Zhao, J. H. Liang, A. M. Zhao, J. T. Liang, D. Tang, Y. P. Gao, J. Alloy. Compd. 691 (2017) 51-59.
[15] D. Dyson, B. Holmes, J. Iron Steel Inst. 208 (1970) 469-474.
[16] N. Van Dijk, A. Butt, L. Zhao, J. Sietsma, S. Offerman, J. Wright, S. Van der Zwaag, Acta Mater. 53 (2005) 5439-5447.
[17] P. Scherrer, Kolloidchemie Ein Lehrbuch, Springer, Berlin Heidelberg, 1912, pp. 387-409.
[18] I. Timokhina, P. Hodgson, E. Pereloma, Metall. Mater. Trans. A 35 (2004) 2331-2341.
[19] W. Li, H. Gao, H. Nakashima, S. Hata, W. Tian, Mater. Sci. Eng. A 649 (2016) 417-425.
[20] X. Xiong, B. Chen, M. Huang, J. Wang, L. Wang, Scripta Mater. 68 (2013) 321-324.
[21] N. Maheswari, S. G. Chowdhury, K. H. Kumar, S. Sankaran, Mater. Sci. Eng. A 600 (2014) 12-20.
[22] R. Ding, D. Tang, A. Zhao, Scripta Mater. 88 (2014) 21-24.
[23] X. L. Zhao, Y. J. Zhang, C. W. Shao, W. J. Hui, H. Dong, J. Iron Steel Res. Int. 24 (2017) 830-837.
[24] A. Ramazani, H. Quade, M. Abbasi, U. Prahl, Mater. Sci. Eng. A 651 (2016) 160-164.